

2015

Effects of Climate Oscillations on Wind Resource Variability in the United States

B. D. Hamlington

Old Dominion University, bhamling@odu.edu


P. E. Hamlington

S. G. Collins

S. R. Alexander

K.-Y. Kim

Follow this and additional works at: https://digitalcommons.odu.edu/ccpo_pubs

 Part of the [Atmospheric Sciences Commons](#), [Climate Commons](#), [Meteorology Commons](#), and the [Oceanography Commons](#)

Repository Citation

Hamlington, B. D.; Hamlington, P. E.; Collins, S. G.; Alexander, S. R.; and Kim, K.-Y., "Effects of Climate Oscillations on Wind Resource Variability in the United States" (2015). *CCPO Publications*. 112.
https://digitalcommons.odu.edu/ccpo_pubs/112

Original Publication Citation

Hamlington, B.D., Hamlington, P.E., Collins, S.G., Alexander, S.R., & Kim, K.Y. (2015). Effects of climate oscillations on wind resource variability in the United States. *Geophysical Research Letters*, 42(1), 145-152. doi: 10.1002/2014gl062370

RESEARCH LETTER

10.1002/2014GL062370

Key Points:

- Cyclostationary empirical orthogonal functions are applied to U.S. wind data
- Climate signal effects on spatial and temporal wind variabilities are identified
- Annual and interannual climate variabilities affect wind sites by up to 30%

Supporting Information:

- Readme
- Text S1
- Figure S1

Correspondence to:

P. E. Hamlington,
peh@colorado.edu

Citation:

Hamlington, B. D., P. E. Hamlington, S. G. Collins, S. R. Alexander, and K.-Y. Kim (2015), Effects of climate oscillations on wind resource variability in the United States, *Geophys. Res. Lett.*, *42*, 145–152, doi:10.1002/2014GL062370.

Received 1 NOV 2014

Accepted 10 DEC 2014

Accepted article online 12 DEC 2014

Published online 9 JAN 2015

Effects of climate oscillations on wind resource variability in the United States

B. D. Hamlington¹, P. E. Hamlington², S. G. Collins², S. R. Alexander², and K.-Y. Kim³

¹Department of Ocean, Earth and Atmospheric Sciences, Old Dominion University, Norfolk, Virginia, USA, ²Department of Mechanical Engineering, University of Colorado Boulder, Boulder, Colorado, USA, ³School of Earth and Environmental Sciences, Seoul National University, Seoul, South Korea

Abstract Natural climate variations in the United States wind resource are assessed by using cyclostationary empirical orthogonal functions (CSEOFs) to decompose wind reanalysis data. Compared to approaches that average climate signals or assume stationarity of the wind resource on interannual time scales, the CSEOF analysis isolates variability associated with specific climate oscillations, as well as their modulation from year to year. Contributions to wind speed variability from the modulated annual cycle (MAC) and the El Niño–Southern Oscillation (ENSO) are quantified, and information provided by the CSEOF analysis further allows the spatial variability of these effects to be determined. The impacts of the MAC and ENSO on the wind resource are calculated at existing wind turbine locations in the United States, revealing variations in the wind speed of up to 30% at individual sites. The results presented here have important implications for predictions of wind plant power output and siting.

1. Introduction

Between 2009 and 2013, wind turbine construction accounted for roughly 30% of new energy capacity installed in the United States, and energy produced from wind now comprises approximately 3–4% of the United States energy portfolio [*American Wind Energy Association*, 2013]. Although the total amount of available wind resource is of substantial concern when siting new wind plants, understanding the temporal variability of this resource is of nearly equal importance, particularly for financing, insurance, and predictions of power output. Changes in the temporal variability at different locations should also be taken into account; this information is critical for understanding the extent to which wind measurements at one location can be applied at another location, as well as for siting wind plants such that the total power production in a particular region is not susceptible to a single climatic event, such as a strong El Niño. In the present study, cyclostationary empirical orthogonal functions (CSEOFs) are, for the first time, used to assess the variability of the wind resource on annual to interannual (i.e., multiyear) time scales at all locations in the United States.

Much of the current understanding of interannual wind resource variability is based on relatively short duration wind speed measurements at existing and prospective wind plant sites, or on data from numerical weather prediction (NWP) and global and regional climate models (GCMs and RCMs, respectively). In general, however, 1 or 2 years of on-site wind speed measurements do not provide a sufficiently long data record to accurately predict wind plant production at a given location [*Ramsdell et al.*, 1980; *Gerdes and Strack*, 1999; *Lackner et al.*, 2008], and some studies have suggested that at least 10 years of data are necessary [*Nfaoui et al.*, 1998; *Landberg et al.*, 2003]. Typically, records of such length do not exist for prospective sites.

Measure-correlate-predict (MCP) methods offer a practical approach to dealing with short data records, and they have consequently become prevalent in the wind industry [*Carta and Velázquez*, 2011; *Carta et al.*, 2013; *Bechrakis et al.*, 2004; *Landberg et al.*, 2003]. These methods attempt to correlate short-term data records at candidate sites with data available from nearby weather stations, which have much longer records. These correlations are then used to generate long-term hindcasts of wind speed data at candidate sites.

A major assumption underlying MCP methods is that wind speed data are statistically stationary throughout the lifetime of the wind project [*Carta et al.*, 2013; *Brower*, 2006] and that the historical distribution of wind speeds will therefore propagate unchanged into the future. This assumption is questionable since the

duration of most on-site wind data records is short relative to the period of low-frequency climate oscillations such as the El Niño-Southern Oscillation (ENSO). It is thus reasonable to expect that wind speed statistics may undergo unanticipated shifts or oscillations during the lifetime of a wind project. It has been shown [Harper, 2005], for example, that strong El Niño events correspond to noticeable reductions in the power production of four wind farms in South Dakota. MCP methods also assume a statistical correlation between the wind resource at prospective sites and nearby weather stations. Recently, however, it was found (M. C. Brower et al., A study of wind speed variability using global reanalysis data, <https://www.awstruepower.com/assets/A-Study-of-Wind-Speed-Variability-Using-Global-Reanalysis-Data2.pdf>, 2013) that wind speed variability can change significantly at locations separated by relatively short distances.

Wind resource assessments using NWP, RCMs, GCMs, and reanalysis data provide a possible solution to the shortcomings associated with MCP. Such data have been used with some success for the study of long-term variations in the wind resource over the United States [Breslow and Sailor, 2002; Pryor et al., 2009], parts of Europe [Pryor et al., 2005; Cradden et al., 2014], and the entire globe [Archer and Jacobson, 2013]. While these studies have provided valuable insights, however, identifying the effects of long-period natural internal climate oscillations such as ENSO or the modulation of the annual cycle requires a data decomposition that allows specific climate signals to be isolated. Interannual variations of the annual cycle, in particular, arise since incident solar radiation on the Earth is not purely periodic and exhibits longer period fluctuations [Wu et al., 2008; Meehl et al., 2009]. It is not uncommon, for example, to experience an unusually cool summer followed by a warmer than normal winter and another cool summer, which would constitute a weaker than normal annual cycle. The existence of a modulated annual cycle (MAC) exhibiting interannual variations in amplitude has been recognized in other climate studies [Kim and Chung, 2001; Wu et al., 2008] and can have a substantial impact on wind resource availability beyond even the well-understood seasonal variations.

CSEOFs provide an ideal framework for determining the temporal and spatial variabilities of the wind resource due to the MAC, ENSO, and other climate oscillations. CSEOFs have been used previously to examine spatial and temporal variations in sea surface height on interannual time scales [Hamlington et al., 2011, 2012, 2014], and in the present study they are used to decompose wind reanalysis data. Using the CSEOF analysis, the maximum and minimum combined effects of the MAC and ENSO are quantified, and the implications of these extrema for the available wind resource are identified at existing wind turbine locations in the United States. This analysis provides a comprehensive picture of the spatial variability of MAC and ENSO effects on the United States wind resource, and the future role of CSEOFs in predictions of wind plant power output and siting is outlined.

2. Cyclostationary Empirical Orthogonal Function Analysis

In order to extract the variability associated with the MAC and ENSO in the United States, a CSEOF analysis [Kim et al., 1996; Kim and North, 1997] is applied to monthly averaged wind speed data. The CSEOF method decomposes space-time data into a series of modes composed of a spatial component (known hereafter as the loading vector (LV)) and a corresponding temporal component (known as the principal component time series (PCTS)). The LVs are spatial maps with physical dimensions (m/s in the present analysis) that, when multiplied by the nondimensional PCTS, give different CSEOF modes for the wind speed distribution. The primary difference between the CSEOF technique when compared to more traditional eigenvalue analyses is that CSEOF LV maps are time varying over a specified nested period. That is, the LVs are spatial maps which capture the temporal evolution related to an inherent physical process, while the corresponding PCTS explains the amplitude of the physical process through time. Larger values of the PCTS indicate increased strength of the physical process at a particular time, while decreased values indicate a weakening of the process. CSEOFs thus provide significant advantages when compared to the more widely used empirical orthogonal functions (EOF), since they avoid the assumption of stationarity in the decomposed spatial patterns and eliminate or reduce the mixing of physical signals across several modes, as frequently occurs in analyses based on EOFs.

The nested period of the CSEOF analysis is selected a priori, with the choice of period usually based on physical understanding or intuition regarding the data to be studied. When studying the annual signal known to be present in many geophysical data sets, for instance, a nested period of 1 year is chosen. Each of the resulting LVs then consists of 12 spatial maps (when using monthly data) that describe the physical evolution of the annual cycle throughout the year. The corresponding PCTS describes the amplitude change, or strength, of the annual cycle from year to year. Additional, much more extensive details on the algorithms

and numerical procedures underlying CSEOF analyses are provided in *Kim et al.* [1996], *Kim and North* [1997], and *Hamlington et al.* [2011].

In recent years, CSEOFs have been increasingly used for the study of climate oscillations and physical processes in the Earth system across a range of time scales and climate variables [*Kim and Chung*, 2001; *Hamlington et al.*, 2011, 2012, 2014; *Yeo and Kim*, 2014]. In such studies, the PCTS from the CSEOF analysis is often compared with climatic indices such as the Multivariate ENSO Index (MEI) in order to identify the contribution of known climate oscillations to the temporal variability of a particular physical quantity. A similar approach is taken in the present study, where the quantity examined is the wind speed and LV maps provided by the analysis are used to determine the spatial distribution of interannual variations in the wind resource.

3. CSEOF Decomposition of Wind Speed

In the present study, the CSEOF analysis is performed on the NCEP North American Regional Reanalysis (NARR) monthly wind speed data set [*Mesinger et al.*, 2006], which covers the time period from 1979 to 2014. Wind speeds are analyzed at a height of 80 m above the Earth surface, which is a standard hub height for modern horizontal axis wind turbines. Data in the NARR data set are provided at specified geopotential pressure levels and have been interpolated to 80 m. While providing a shorter data record than other reanalysis products, the spatial resolution (roughly 0.5°) of this data set is relatively high.

A 1 year nested period is used for the CSEOF analysis. The 1 year nested period has been selected to target the MAC, a primary signal of interest in this study. In previous studies, a 1 year nested period has also been shown to be suitable and used to extract the variability associated with ENSO [e.g., *Kim and Chung*, 2001; *Hamlington et al.*, 2011]. While a 2 year nested period may be more appropriate for capturing the biennial oscillation from warm to cold phase in addition to the lower frequency variability of ENSO (see *Yeo and Kim* [2014], for example), the 1 year nested period coupled with a simple CSEOF regression technique (discussed in more detail below) is appropriate for capturing the ENSO-related wind speed variability over the United States. Prior to performing the CSEOF decomposition, wind speed anomalies are calculated by removing the mean and linear trends from each point in space. As a result, the subsequent CSEOF modes represent departures from the mean field; negative values in the CSEOF modes represent reductions in the wind speed relative to the mean, while positive values represent increases relative to the mean.

The LVs and PCTS for the first mode resulting from the wind speed anomaly CSEOF decomposition are shown in Figure 1. This mode describes over 50% of the variability in the data set, as determined by the first eigenvalue of the CSEOF decomposition. Following the analysis in *Kim and Chung* [2001] and *Wu et al.* [2008], this mode represents the MAC since the PCTS in Figure 1 (bottom row) is strictly positive, thus indicating that the physical period of the first-mode signal is fully described by the temporal variation of the 12 LV maps contained within the 1 year, or annual, nesting. A simple and intuitive justification for this conclusion is provided, for example, through consideration of the hypothetical surface temperature: with a 1 year nested period, the temperature transition from winter to summer and back to winter would be captured in the LVs, but if the PCTS were to change sign, this would imply that winter and summer had “reversed” their identities. The strictly positive nature of the PCTS thus ensures that the LV describes variability with a 1 year period. In Figure 1, the LV maps describing the spatial patterns of the MAC in wind speed anomaly are shown in the top and middle rows (averaged monthly according to the corresponding labels in order to produce one map for each season), while the bottom row shows the PCTS describing the amplitude modulation of the annual cycle from year to year. As further evidence that this mode represents the MAC, the PCTS and LVs can be recombined, and by computing the mean over the region of interest, the 1 year period of the signal becomes clear (see Figure S1 in the supporting information).

The LV maps in Figure 1 show that, for much of the country, wind speeds are highest in the winter when the poleward temperature and pressure gradients are strongest, and that the lowest wind speeds occur during the summer. Examining the spatial patterns further, the highest wind speeds resulting from the annual cycle occur during the winter in the northwestern United States and extend down through the Rocky Mountain region. In general, the LV maps obtained from the CSEOF analysis for the first (i.e., MAC) mode are consistent with results from studies performed at specific sites [e.g., *Klink*, 1999], thus providing additional verification that the first mode is related to the annual cycle.

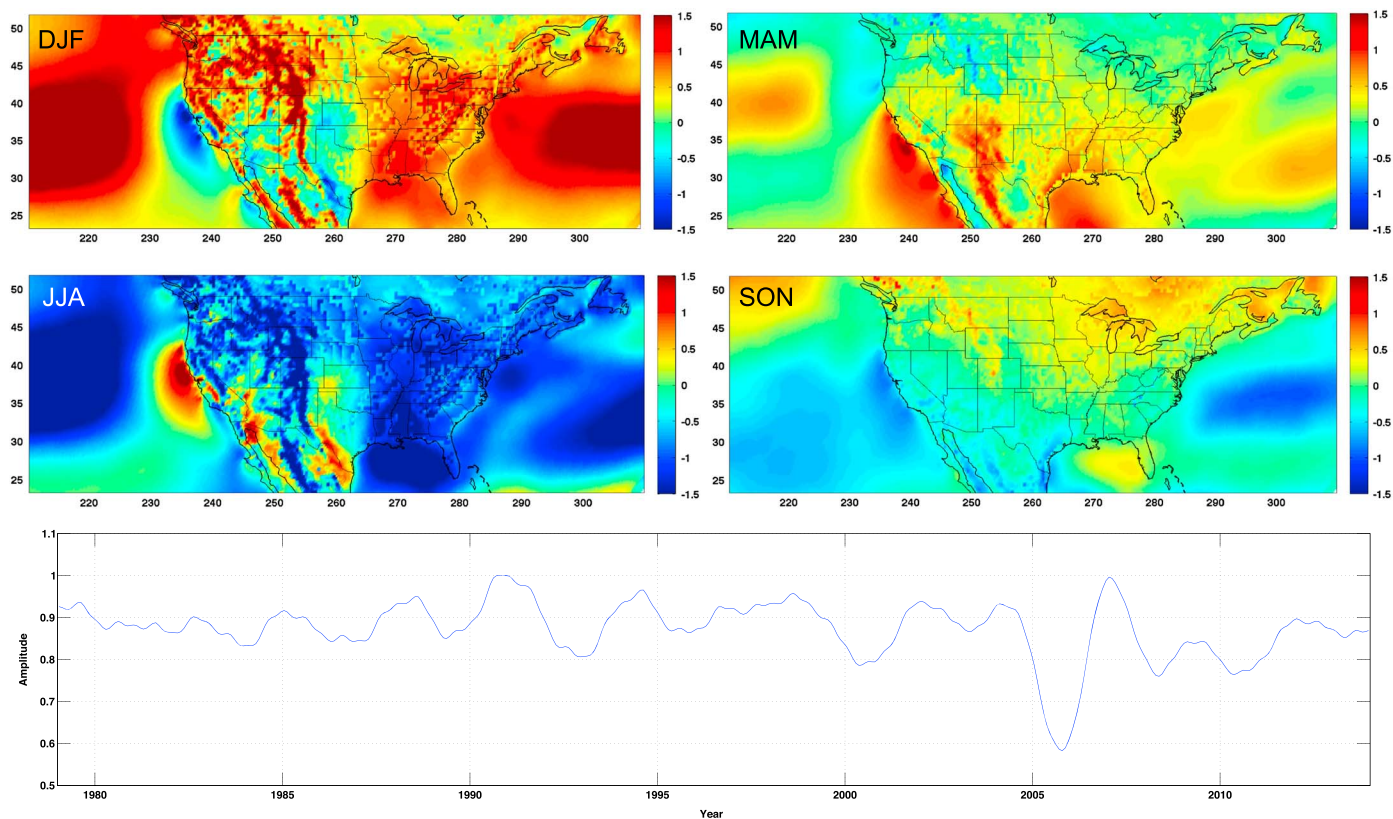


Figure 1. Mode 1 of the CSEOF decomposition, explaining the MAC, after removing the long-term trend for the NARR near-surface wind speed data set so that the CSEOF analysis is performed on the wind speed anomaly. (top and middle rows) LVs (units of m/s, averaged monthly according to the labels to produce one map for each season) and (bottom row) PCTS (dimensionless), representing the interannual amplitude modulation of the annual cycle, are shown.

The CSEOF analysis further indicates how the strength of the annual cycle varies from year to year. The PCTS in Figure 1 (bottom row) shows that the strength of the annual cycle in the United States can differ by over 25%. Most notably, the strength of the annual cycle from 2005 to 2006 decreased by approximately 30% which, when coupled with the LV maps in Figure 1 (top and middle rows), represents a significant change in the wind resource availability for many areas of the country.

In prior studies of sea level or sea surface temperature [Hamlington *et al.*, 2011, 2012], the second mode of the CSEOF decomposition was generally found to describe ENSO-related variability. In the CSEOF wind speed anomaly decomposition performed here, the second mode describes 5% of the variance in the data set. As a first step in determining if the mode is related to ENSO, the second-mode PCTS is correlated with the MEI [Wolter and Timlin, 2011], giving a correlation coefficient of 0.58 over the entire 35 year data record. As discussed in Yeo and Kim [2014], however, a longer data record is typically needed to fully capture the ENSO variability with a single mode.

In order to alleviate some of the challenges posed by the relatively short data record studied here, a simple CSEOF regression technique (described in more detail in Hamlington *et al.* [2012] and used in recent studies such as Yeo and Kim [2014]) is used to reduce mode mixing and improve the representation of ENSO variability by a single mode. The PCTS from the CSEOF decomposition of the wind speed anomaly is regressed onto the MEI to obtain a set of regression coefficients, one for each of the modes used in the regression. The first 18 modes are used (excluding the MAC mode) corresponding to a little less than 40% of the variance in the original data. The number of modes used is determined based on overfitting criteria and a simple F test. These regression coefficients are then multiplied by each corresponding LV obtained from the wind speed anomaly CSEOF decomposition prior to the regression (further details are provided in the supporting information). This creates a single wind speed anomaly LV with temporal evolutions described by the MEI. That is, the regression technique is used to create a LV with an accompanying PCTS that corresponds to the MEI. The resulting CSEOF mode is shown in Figure 2, with the top and middle rows providing seasonal

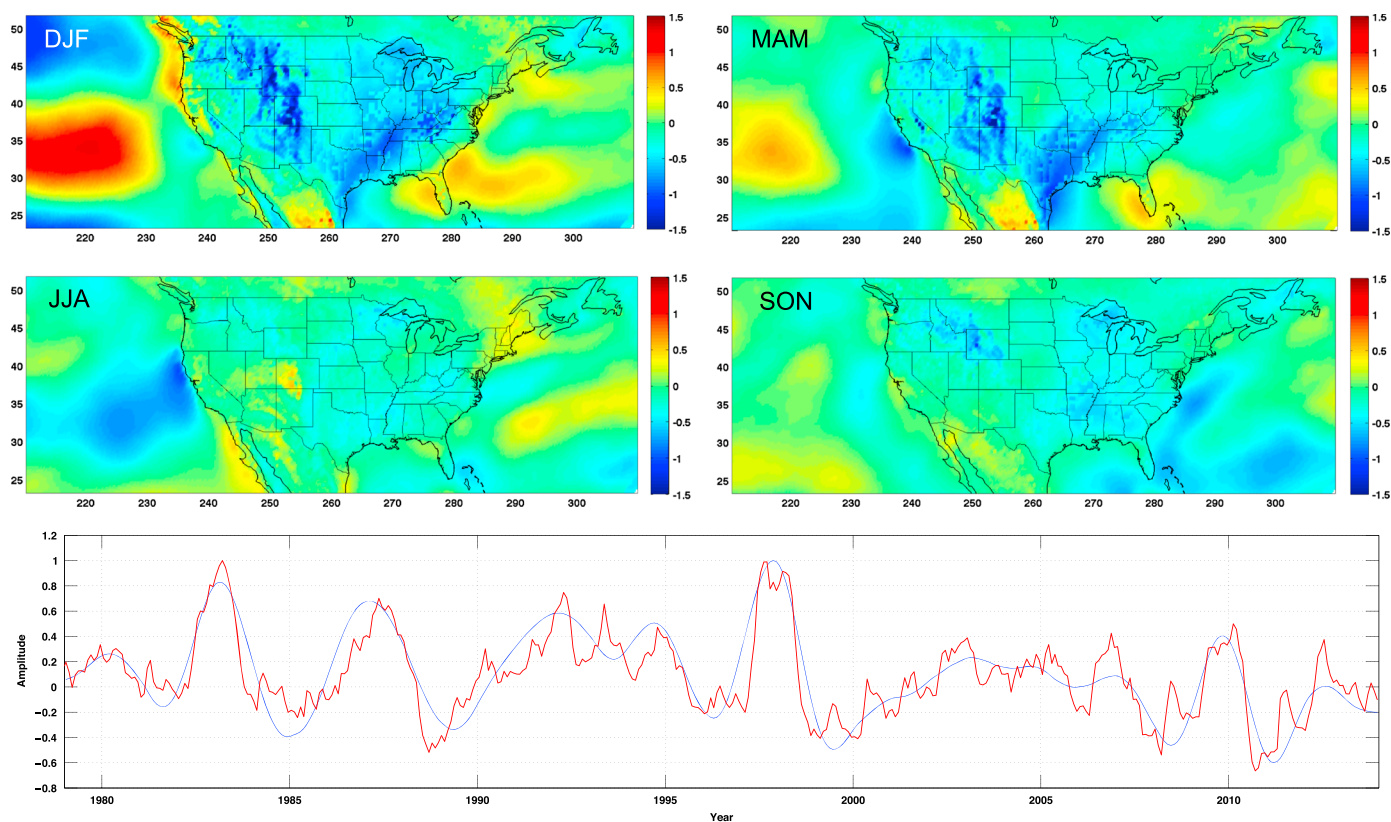


Figure 2. Regressed CSEOF mode of the near-surface wind speed anomaly data set representing the variability associated with ENSO. (top and middle rows) LVs (units of m/s averaged monthly according to the labels to produce one map for each season) and (bottom row) PCTS (dimensionless) are shown. The Multivariate ENSO Index (MEI; red) is plotted with the PCTS (blue) to demonstrate the relationship between the mode and ENSO. The LV maps depict the positive phase of ENSO.

spatial patterns describing ENSO-related wind speed variations, and the bottom row showing the PCTS and the MEI.

The LV maps shown in Figure 2 indicate that during an El Niño event (corresponding to positive values of the PCTS), wind speed anomalies obtained by multiplying the PCTS and LVs are strongly negative in a large portion of the country during the winter and spring seasons, particularly through the western Great Plains and up through the Ohio River Valley. This is, in turn, indicative of a suppression of the wind speed in these regions during an El Niño event. Conversely, during a La Niña event (corresponding to negative values of the PCTS), the opposite effect is observed, with a positive wind speed anomaly and increased wind speeds through much of the country during the winter and spring. The effect of ENSO on the wind speed over the continental United States is smaller yet still significant (roughly 1 m/s in some regions) in the summer and fall.

Previous studies have established that ENSO is teleconnected to storm tracks over North America, particularly during the winter and spring [Horel and Wallace, 1981; Wallace and Gutzler, 1981]. Enloe *et al.* [2004] extended these studies by examining the impact of ENSO on peak wind gusts at specific locations across the United States and were able to relate the shift in storm tracks to changes in peak wind gusts. During an El Niño event, the storm track is shifted to the south and flattened. Following the discussion in Enloe *et al.* [2004], this leads to decreased winds for much of the central and northern United States, as can also be seen in the spatial patterns in Figure 2. Agreeing with the analysis in Enloe *et al.* [2004], the opposite effect occurs during a La Niña event. St. George and Wolfe [2009] also found that El Niño reduces winter winds in the southern Canadian Prairies, consistent with the results shown here. Once again, therefore, the LVs and PCTS in Figure 2 are consistent with the relatively limited observations of ENSO-related variability from prior studies, while at the same time providing more comprehensive coverage of this variability over the entire United States.

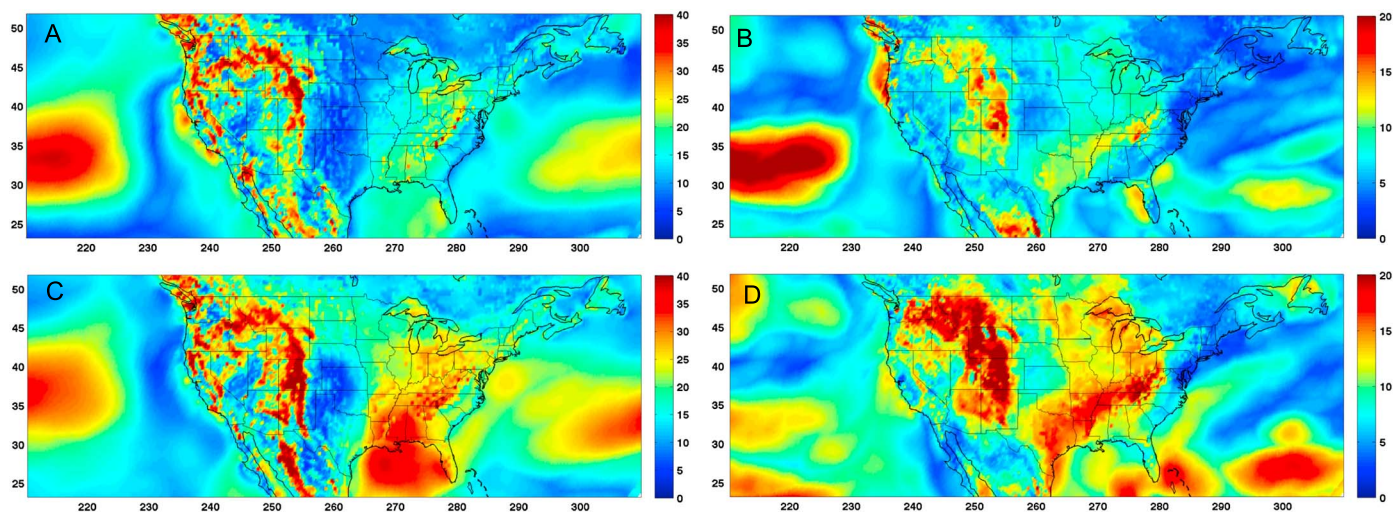


Figure 3. Maximum percentage increase and decrease in the wind speed anomaly relative to the long-term mean for the (a and c) MAC (increase and decrease, respectively) and (b and d) ENSO (increase and decrease, respectively), as given by the modes shown in Figures 1 and 2.

4. Discussion and Conclusions

With the first and the regression-reconstructed second CSEOF modes representing the MAC- and ENSO-related wind speed variabilities, it is possible to begin an assessment of the effects of climatic oscillations on the wind resource across the United States. To understand the range of potential impacts resulting from MAC and ENSO variabilities, the maximum percentage increase and decrease in the wind speed relative to the long-term mean is computed. Figure 3 shows the largest percentage increase and decrease observed in the 35 year record relative to the mean wind speed for the MAC and ENSO. The MAC can cause changes in the wind speed (both increasing and decreasing) greater than 40%, with the western United States particularly affected. By examining the areas of maximum variability in Figure 2, the region of increased wind speed in the Great Plains shown in Figure 3b corresponds to the cold phase of ENSO (i.e., La Niña). In other words, when the PCTS is negative indicating a La Niña, the contribution to wind speed in the Great Plains that is negative in the winter LV maps becomes positive. Similarly, comparison with Figure 2 indicates that the substantial suppression of wind speed in the Great Plains shown in Figure 3d corresponds to the warm phase of ENSO (i.e., El Niño). The increase in wind resource off the northwestern coast of the United States, shown in Figure 3b, is connected with the warm phase of ENSO using similar reasoning.

From the maps shown in Figure 3, the effects of the MAC and ENSO can be determined at specific wind turbine locations in the United States. Figure 4a shows the locations of more than 34,000 onshore wind turbines with hub heights of at least 50 m, as provided by the United States Geological Survey [Diffendorfer *et al.*, 2014]. The maps of spatial variability in Figure 3 are subsampled at each of these locations to produce histograms of the maximum percentage increase and decrease in wind speed resulting from the MAC (Figure 4b), ENSO (Figure 4c), and the combination of the two modes (Figure 4d). While active wind plants are generally not located in the areas of highest variability associated with the MAC and ENSO, the wind speed percentage increase and decrease approaches 30% for the MAC and 20% for ENSO, which is significant when considering the long-term impact on the availability of wind resources. It should be noted that the wind speed histograms in Figure 4 are calculated without regard to the power output of specific turbines (i.e., 50 kW turbines are treated in the same way as 1.5 MW turbines). In the future, these histograms may be weighted by the capacities of the individual turbines or even by the expected output calculated using turbine power curves.

Maps such as those in Figure 3 and statistics such as those in Figure 4 can substantially aid in the understanding and prediction of uncertainty, variability, and total power output of current and future United States wind energy capacity. In addition to maps of maximum percentage increase and decrease, the standard deviation of the wind speed can also be computed, providing a direct measure of the uncertainty at a particular wind site over interannual time scales. Moreover, using the CSEOF analysis this uncertainty can be attributed to particular climate signals such as the MAC or ENSO.

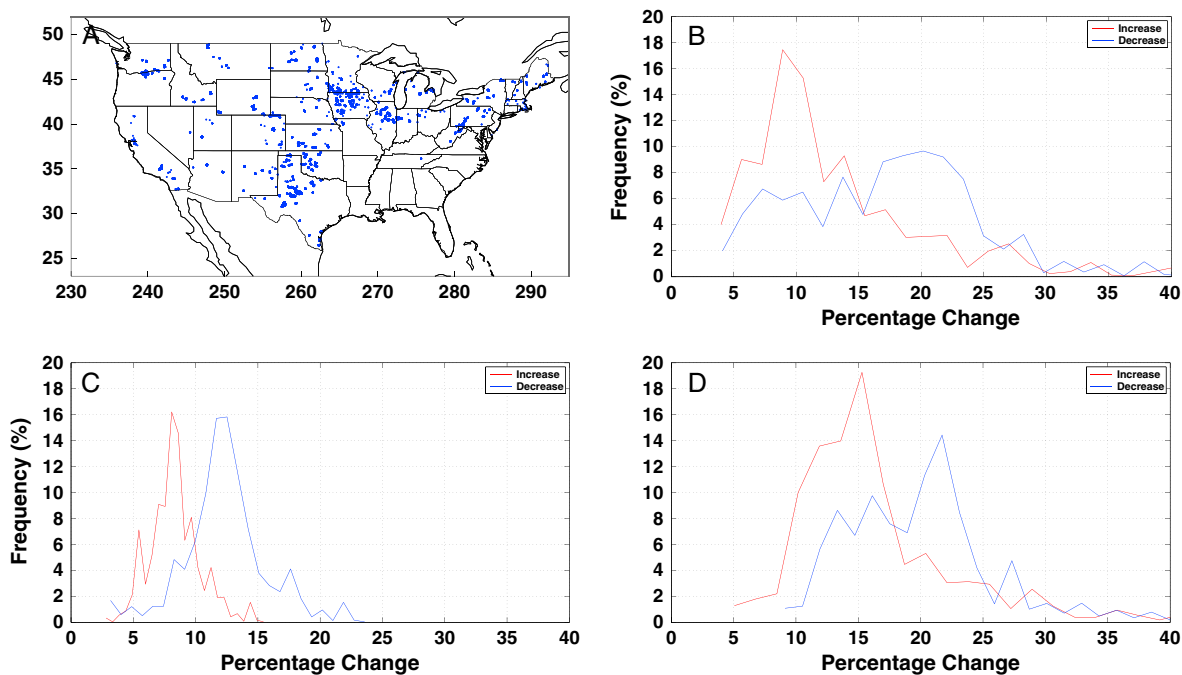


Figure 4. Maximum percentage increase and decrease in wind speed anomaly relative to the long-term mean over the full 35 year record at (a) wind turbine locations for (b) the MAC mode, (c) ENSO mode, and (d) the combination of both modes.

Coupled to the analysis of uncertainty and variability, the assumptions underlying MCP methods may also be tested using the CSEOF analysis. By identifying and mapping sites where wind speed statistics vary significantly with known climatic oscillations, CSEOFs provide a means of validating or rejecting the fundamental assumptions of MCP methods. In particular, the assumption of a high spatial correlation between wind sites and nearby weather stations can be tested (provided that reanalysis data are available with sufficiently high spatial resolution), as can the assumed statistical stationarity of the wind resource over interannual timescales.

Finally, LVs and uncertainty maps such as those in Figures 1–3 can aid in siting of new wind plants by identifying locations with either a strong or weak, negative or positive, dependence on specific climate signals. With maps such as those in Figures 1 or 2, in particular, it is possible to identify complementary wind sites with negative spatial correlation such that a particular climatic event (e.g., a strong El Niño event) will have a positive effect on the wind speed at one site and a negative effect at another site, thus leaving the overall resource across the two sites relatively constant.

Given longer data records, the CSEOF analysis outlined here could be applied to the United States wind resource in order to identify decadal and multidecadal trends, including long-term trends due to climate change. Rather than using simply reanalysis data, the CSEOF analysis could also be applied equally well to existing and new computational data from NWP simulations, RCMs, and GCMs. It should be noted that the present study has only examined the wind speed variability at specific wind turbine locations; in the future, the measured variations could be passed through real or representative wind turbine power curves in order to obtain more direct assessments of the impact of ENSO and the MAC on the power output of installed and prospective wind energy capacity. Finally, the present CSEOF analysis provides the spatial variation of the MAC and ENSO climate signals, but further study is required in order to determine the physical reasons (e.g., geography) for these variations.

References

Archer, C. L., and M. Z. Jacobson (2013), Geographical and seasonal variability of the global “practical” wind resources, *Appl. Geo.*, *45*, 119–130.
 American Wind Energy Association (2013). [Available at <http://www.awea.org>.]
 Bechrakis, D. A., J. P. Deane, and E. J. McKeogh (2004), Wind resource assessment of an area using short term data correlated to a long term data set, *Sol. Energy*, *76*, 725–732.

Acknowledgments

Helpful discussions with Ryan King are gratefully acknowledged. B.D.H. was supported by NASA grants NNX11AE26G and NNX13AH05G and S.G.C. was supported by a Discovery Learning Apprenticeship (DLA) at the University of Colorado, Boulder. K.Y.K. acknowledges support from SNU-Yonsei Research Cooperation Program through Seoul National University (SNU) in 2014. NARR Reanalysis data were provided by the NOAA/OAR/ESRL PSD, Boulder, Colorado, USA, from their website at <http://www.esrl.noaa.gov/psd/>.

The Editor thanks two anonymous reviewers for their assistance in evaluating this paper.

- Breslow, P. B., and D. J. Sailor (2002), Vulnerability of wind power resources to climate change in the continental United States, *Renewable Energy*, *27*, 585–598.
- Brower, M. C. (2006), The use of NCEP/NCAR Reanalysis data in MCP, Session DT1, European Wind Energy Conference and Exhibition, Athens, Greece, 27 Feb–2 Mar.
- Carta, J. A., and S. Velázquez (2011), A new probabilistic method to estimate the long-term wind speed characteristics at a potential wind energy conversion site, *Energy*, *36*, 2671–2685.
- Carta, J. A., S. Velázquez, and P. Cabrera (2013), A review of measure-correlate-predict (MCP) methods used to estimate long-term wind characteristics at a target site, *Renewable Sustainable Energy Rev.*, *27*, 362–400.
- Cradden, L. C., F. Restuccia, S. L. Hawkins, and G. P. Harrison (2014), Consideration of wind speed variability in creating a regional aggregate wind power time series, *Resources*, *3*, 215–234.
- Diffendorfer, J. E., R. Compton, L. Kramer, Z. Ancona, and D. Norton (2014), Onshore industrial wind turbine locations for the United States, U.S. Geological Survey Data Series 817.
- Enloe, J., J. J. O'Brien, and S. R. Smith (2004), ENSO impacts on peak wind gusts in the United States, *J. Clim.*, *17*, 1728–1737.
- Gerdes, G., and M. Strack (1999), Long-term correlation of wind measurement data, *DEWI*, *15*, 18–24.
- Hamlington, B. D., R. R. Leben, R. S. Nerem, W. Han, and K.-Y. Kim (2011), Reconstructing sea level using cyclostationary empirical orthogonal functions, *J. Geophys. Res.*, *116*, C12015, doi:10.1029/2011JC007529.
- Hamlington, B. D., R. R. Leben, and K.-Y. Kim (2012), Improving sea level reconstructions using non-sea level measurements, *J. Geophys. Res.*, *117*, C10025, doi:10.1029/2012JC008277.
- Hamlington, B. D., M. W. Strassburg, R. R. Leben, W. Han, R. S. Nerem, and K.-Y. Kim (2014), Uncovering an anthropogenic sea-level rise signal in the Pacific Ocean, *Nat. Clim. Change*, *4*, 782–785.
- Harper, B., (2005), ENSO's effect on the wind energy production of South Dakota, *Technical Report*, Univ. Corp. for Atmos. Res., Boulder, Colo.
- Horel, J. D., and J. M. Wallace (1981), Planetary-scale atmospheric phenomena associated with the Southern Oscillation, *Mon. Weather Rev.*, *109*, 813–829.
- Kim, K.-Y., G. R. North, and J. Huang (1996), EOFs of one-dimensional cyclostationary time series: Computations, examples, and stochastic modeling, *J. Atmos. Sci.*, *53*, 1007–1017.
- Kim, K. Y., and G. R. North (1997), EOFs of harmonizable cyclostationary processes, *J. Phys. Oceanogr.*, *54*, 2416–2427.
- Kim, K. Y., and C. Chung (2001), On the evolution of the annual cycle in the tropical Pacific, *J. Clim.*, *14*, 991–994.
- Klink, K. (1999), Climatological mean and interannual variance of United States surface wind speed, direction, velocity, *Int. J. Climatol.*, *19*, 471–488.
- Lackner, M. A., A. L. Rogers, and J. F. Manwell (2008), Uncertainty analysis in MCP-based wind resource assessment and energy production estimation, *J. Sol. Energy Eng.*, *130*, 031006.
- Landberg, L., L. Mylnerup, O. Rathmann, E. L. Petersen, B. H. Jorgensen, and B. J. Niels (2003), Wind resource estimation: An overview, *Wind Energy*, *6*, 261–271.
- Meehl, G. A., J. M. Arblaster, K. Matthes, F. Sassi, and H. van Loon (2009), Amplifying the Pacific climate system response to a small 11-year solar cycle forcing, *Science*, *325*, 1114–1118.
- Mesinger, F., et al. (2006), North American regional reanalysis, *Bull. Am. Meteorol. Soc.*, *87*, 343–360.
- Nfaoui, H., J. Buret, and A. A. M. Sayigh (1998), Wind characteristics and wind energy potential in Morocco, *Sol. Energy*, *63*, 51–60.
- Pryor, S. C., R. J. Barthelmie, and E. Kjellström (2005), Potential climate change impact on wind energy resources in northern Europe: Analyses using a regional climate model, *Clim. Dyn.*, *25*, 815–835.
- Pryor, S. C., R. J. Barthelmie, D. T. Young, E. S. Takle, R. W. Arritt, D. Flory, W. J. Gutowski Jr., A. Nunes, and J. Roads (2009), Wind speed trends over the contiguous United States, *J. Geophys. Res.*, *114*, D14105, doi:10.1029/2008JD011416.
- Ramsdell, J. V., S. Houston, and H. L. Wegley (1980), Measurement strategies for estimating long-term average wind speeds, *Sol. Energy*, *25*, 495–503.
- St. George, S., and S. A. Wolfe (2009), El Niño stills winter winds across the southern Canadian Prairies, *Geophys. Res. Lett.*, *36*, L23806, doi:10.1029/2009GL041282.
- Wallace, J. M., and D. S. Gutzler (1981), Teleconnections in the geopotential height field during the Northern Hemisphere winter, *Mon. Weather Rev.*, *109*, 784–811.
- Wolter, K., and M. S. Timlin (2011), El Niño/Southern Oscillation behavior since 1871 as diagnosed in an extended multivariate ENSO index (MEI.ext), *Int. J. Climatol.*, *31*, 1074–1087.
- Wu, Z., E. K. Schneider, B. P. Kirtman, E. S. Sarachik, N. E. Huang, and C. J. Tucker (2008), The modulated annual cycle: An alternative reference frame for climate anomalies, *Clim. Dyn.*, *31*, 823–841.
- Yeo, S. R., and K. Y. Kim (2014), Global warming, low-frequency variability and biennial oscillation: An attempt to understand the physical mechanisms driving major ENSO events, *Clim. Dyn.*, *43*, 771–786.